Role of extracellular polymeric substances (EPS) from *Pseudomonas putida* strain MnB1 in dissolution of natural rhodochrosite

H.W. Wang[1, 2] G. M. Gadd [1, 3] D. Y. Zhang[1,4] and X.L. Pan[1*]

[1] Xinjiang Key Laboratory of Environmental Pollution and Bioremediation, Xinjiang Institute of Ecology and Geography, Chinese Academy of Sciences, Urumqi 830011, China

[2] University of Chinese Academy of Sciences, Beijing, 100049, China

[3] Geomicrobiology Group, College of Life Science, University of Dundee, Dundee DDI 5 EH, Scotland, UK

[4] State Key Laboratory of Environmental Geochemistry, Institute of Geochemistry, Chinese Academy of Sciences, Guiyang 550002, China

Correspondence to: X. Pan (panxl@ms.xjb.ac.cn)

Abstract

Microbially mediated oxidation of Mn(II) to Mn oxides has been demonstrated in previous studies, however, the mechanisms of how bacteria dissolve and oxidize using a solid Mn(II) substrate are poorly understood. In this study, we examined the role of extracellular polymeric substances (EPS) from *Pseudomonas putida* strain MnB1 in enhancing the dissolution of natural rhodochrosite. The results showed that *P. putida* strain MnB1 cells can effectively dissolve natural and synthetic rhodochrosite and subsequently oxidize liberated Mn(II) ions to form Mn oxides, and EPS were found to play an important role in increasing the dissolution of natural rhodochrosite. Compared with EPS-free treatment, the dissolution rate of natural rhodochrosite in the presence of bacterial EPS was significantly increased with decreasing initial pH and increasing EPS concentration, ionic strength and rhodochrosite dosage ($p<0.05$). Fourier-transform infrared spectroscopy (FTIR) analysis implied that functional groups like N-H, C=O and C-H in the EPS contributed to the dissolution of natural rhodochrosite. This study is helpful for understanding the biogeochemical processes involved in the formation of biogenic Mn oxides from a solid Mn(II) substrate.

1 Introduction

Mn oxides are thought to be one of the most important minerals in surface waters (Shiller and Stephens, 2005; Tebo et al., 2005). They are of importance in the cycling of nutrient elements, the transformation of toxic persistent pollutants and the immobilization of heavy metals because of their high reactivity and wide existence in the environment (Tebo et al., 2005; Zhu et al., 2009; Lafferty et al., 2010). Since the 1960s, microbially mediated oxidation of divalent Mn ion to generate Mn oxides was reported, and some relevant mechanisms of Mn oxidation induced by microbes have been illustrated recently (Villalobos et al., 2003; Spiro et al., 2010; Learman et al., 2011a; Learman et al., 2011b; Hansel et al., 2012).

Rhodochrosite is one of the Mn(II) minerals and widely distributed in different

natural environments (Germann, 1973; Okita, 1992; Roy, 1997; Fan and Yang, 1999). Oxidative dissolution of rhodochrosite leads to production of Mn(II) and Mn oxides. The solubility of synthetic rhodochrosite in pure water and saline solution has been reported (Jensen et al., 2002; Luo and Millero, 2003; Duckworth and Martin, 2004;), and rhodochrosite oxidation by O_2 or iron oxides is thermodynamically favourable, but the oxidation rate is rather slow (Diem and Stumm, 1984; Madden and Hochella, 2005). Recently, oxidative dissolution of natural rhodochrosite by Mn(II) oxidizing fungi and the role of extracellular superoxide and organic molecules during Mn oxides formation have been reported (Tang et al., 2013). However, the mechanisms of natural rhodochrosite dissolution by microbes are poorly understood.

Oxidative dissolution of natural rhodochrosite by microbes may link to a dynamic process at solid-liquid interfaces (Pan 2010). For example, the bioleaching of metal sulfide minerals was mediated by a series of interfacial processes such as attachment of cells to surfaces of minerals, dissolution of mineral by bacterial EPS and oxidation of low valency Fe and S (Bosecker, 1997; Gehrke et al., 1998; Fowler et al., 1999; Tributsch, 2001; Rohwerder et al., 2003). Until now, the mechanism of bioleaching is still an open question for researchers. Therefore, studying the interfacial processes between the bacterial EPS layer and the rhodochrosite mineral surface is helpful to understand the mechanism of bacterial oxidation of solid origin Mn(II) and the biogeochemical cycle of Mn.

In this study, the role of EPS in oxidative dissolution of natural rhodochrosite was investigated using a Mn oxidizing bacterium, *Pseudomonas putida* MnB1. The dissolution and oxidation kinetics of rhodochrosite were examined by batch experiments and the products of Mn oxides were analyzed by scanning electron microscopy and energy dispersive spectrometry (SEM-EDS). Moreover, effects of pH, EPS concentration, ion strength and rhodochrosite dosage on the dissolution rate of rhodochrosite in the presence of EPS were also investigated. Functional groups in EPS involved in dissolving rhodochrosite were analyzed by FTIR.

2 Materials and methods

2.1 Culture of Bacterium

The Mn oxidizing bacterium, *Pseudomonas putida* strain MnB1 (ATCC 23483) was used in this study. The *P. putida* MnB1 cells were cultured in the medium under aerobic conditions as reported by Kim et al., (2012), which was composed of 0.5 g L^{-1} of yeast extract, 1 g L^{-1} of glucose, 0.5 g L^{-1} of casamino acids, 0.815 g L^{-1} $MgSO_4$ •$7H_2O$, 0.294 g L^{-1} of $CaCl_2$ •$2H_2O$, 0.001 g L^{-1} $FeCl_3$ •$7H_2O$ and 1ml of trace element solution. The trace element solution was composed of 2.496 g L^{-1} $CuSO_4$ • $5H_2O$, 12.653 g L^{-1} $ZnSO_4$ • $7H_2O$, 4.758 g L^{-1} $CoCl_2$ • $6H_2O$ and 3.145 g L^{-1} Na_2MoO_4 • $2H_2O$. The cells were harvested after two days of culture for further experiments. For batch experiments, *P. putida* MnB1 cells were incubated at 25°C in the #279 medium (ATCC™) containing 0.15 g of $Fe(NH_4)_2(SO_4)_2$ • $6H_2O$, 0.075 g of yeast extract, 0.15 g of sodium citrate, 0.05 g of $Na_4P_2O_7$ • $10H_2O$ in one liter of ultra-purified water with an initial pH of 6.8.

2.2 Preparation of rhodochrosite

Natural rhodochrosite mineral used in this study was collected from a Mn mine near Xiangtan city, Hunan province, China. The mineral samples were dried at ambient temperature and sieved through a 200 mesh nylon screen after grinding. SEM-EDS analysis (Fig. 1a) showed that natural rhodochrosite was mainly composed of O, Mn and C, and other foreign ions such as Al, Mg, S and K. Powder X ray diffraction (XRD) analysis (Fig. 1c) shows that the raw mineral mainly contains rhodochrosite (83.4%) and some quartz (16.6%) with a total Mn content of 201.93 ± 11.42 mg g^{-1}. Prior to batch and other experiments, the samples of natural rhodochrosite were washed three times with ultra-purified water to remove the dissociative Mn(II) used for further experiments. Fresh synthetic rhodochrosite was prepared before experiments by dropwise addition of 2 M NH_4HCO_3 to 1 M $MnSO_4$ • H_2O with vigorous magnetic stirring at ambient temperature. The particles were washed three times with ultra-purified water and then dried for 12h at 85°C. The characteristics of synthetic rhodochrosites were analysed by XRD (Fig. 1 c) and SEM-EDS (Fig. 1b).

2.3 Oxidative dissolution of rhodochrosite by *P. putida* MnB1

Experiments on oxidative dissolution of natural and synthetic rhodochrosite by *P. putida* MnB1 were carried out in 100 ml glass bottles fitted with rubber stoppers. 50 ml of fresh sterilized medium, 0.2 g of natural rhodochrosite and 1 ml of cell suspension pre-cultured for 2 days were added into the glass bottles. The final bacterial cell density was approximately 4×10^7 cells ml^{-1}. Inactivated control was performed using Na_3N treatment (0.3%, wt) to inhibit the biological activity of *P. putida* MnB1. The bottles without cells were used as the sterile control. All the treatments were carried out in triplicate. The bottles were shaken at 120 rpm and 25°C. At different time intervals, concentrations of Mn(II) in solution and Mn oxides were determined accordingly.

2.4 Dissolution of natural rhodochrosite by bacterial EPS

For EPS extraction, cells were grown in the medium at 120 rpm and 25°C for 3 days (OD_{600}=0.8). The method for EPS extraction was slightly modified based on a previous report (Zhang et al., 2013). Briefly, the cell samples were centrifuged at 11600 g for 5 min at 4°C to remove superfluous medium. The pellets were re-suspended in ultra-purified water and centrifuged at 26000 g for 25 min at 4°C. The suspension was collected and filtered through a 0.45 μm acetate cellulose membrane and further purified by 3500 Dalton dialysis membrane for 5 times (every 12 h) at 4°C in the dark. After purification, the characteristics of EPS samples including TOC, proteins, polysaccharides and pH were determined and the results are as follows: TOC, 51 ± 1.52 mg L^{-1}; proteins, 47.03 ± 0.22 μg mL^{-1}; polysaccharides, 11.12 ± 0.04 μg mL^{-1}; and pH 6.8. In addition, dissolved and freeze dried EPS samples were stored at -20°C in the dark for further experiments.

Dissolution of natural rhodochrosite by EPS was carried out in 50 ml Erlenmeyer flasks on a reciprocating shaker at 200 rpm and 25°C. Effect of environmental factors, such as pH, ionic strength, EPS concentration and rhodochrosite dosage were examined. The treatment without addition of EPS was set as the control. The

experimental parameters of the natural rhodochrosite dissolution rate for different treatments are summarized in Table 1. The pH of all test solutions was adjusted by 0.01 M NaOH or HCl and measured by an automatic potentiometric titrator with a pH electrode (Metrohm 702, Switzerland). Different ionic strengths were obtained by addition of different amounts of NaCl. Each experiment was conducted in triplicate. After 360 min reaction, the samples were collected and filtered through 0.22 μm filters for Mn(II) concentration and FTIR analysis. For FTIR analysis, the filtered EPS was directly lyophilized by a vacuum freeze dryer. The dissolution rate of natural rhodochrosite was calculated as follows:

$$k = \frac{C \times V}{T}$$

k: The dissolution rate of natural rhodochrosite (μg Mn(II) min^{-1}); *C*: Mn^{2+} ion concentration in solution after dissolution of natural dissolution (μg Mn(II) L^{-1}); *V*: total volume of experimental solution (L); *T*: dissolution time (min).

2.5 Preparation of Mn oxides for SEM-EDS and XRD analysis

After oxidative dissolution of rhodochrosite experiments, Mn oxides with live cell treatments were collected. Moreover, biogenic Mn oxides, which used dissolved Mn^{2+} ions as the Mn(II) origin, were obtained by oxidizing Mn^{2+} ions (5 mg L^{-1}) in the presence of 50 ml living cells and sterile #279 medium after reaction for 24 h. Before SEM-EDS and XRD analysis, these biogenic Mn oxide samples were washed three times with ultra-purified water and then lyophilized by a vacuum freeze dryer. δ-MnO_2 was synthesized according to a published method (Villalobos et al., 2003).

2.6 Analytical methods

For oxidative dissolution experiments, at different time intervals, 1 ml of samples were collected and centrifuged at 15,600 g for 5 min. The concentration of Mn(II) in the supernatant was analyzed by manganese formaldehyde oxime spectrophotometry (Brewer and Spencer, 1971). The residues were resuspended in 1 ml ultra-purified water and 0.2 ml LBB (wt, 0.04 %) and 3 ml 45 mM acetic acid were added and the

absorbance value at 620 nm was determined for Mn oxides concentration (Okazaki et al., 1997). The standard curves for the LBB colorimetric method were obtained by oxidation of LBB by $KMnO_4$ and the data shown as MnO_2 equivalents.

The content of TOC in EPS samples was determined using a TOC analyzer (Model 1030, Aurora, USA). The polysaccharide content in EPS was determined by the phenol–sulfuric acid method (Saha and Brewer, 1994). The content of protein in EPS was measured using a modified Lowry procedure (Paxman, 1972).

FTIR analysis of EPS samples were recorded using a FTIR spectrophotometer (Vertex 70, Bruker, Germany). Mn oxide samples were sprayed with gold and analyzed by SEM (Zeiss Super 55VP, Germany) coupled with EDS spectroscopy (Bruker XFlash 5010, Germany). XRD spectra were obtained using an X-ray powder diffractometer (Bruker D8, Germany). The components were identified by comparison with standards diffraction data provided by software of Jade 5.0.

2.7 Statistics

Means and standard errors (n=3) were calculated and the significance between control and experimental treatments was obtained using Tukey's test. The significance level was accepted when the value of p was less than 0.05.

3 Results and discussion

3.1 Oxidative dissolution of rhodochrosite by *P. putida* MnB1

Oxidative dissolution of natural rhodochrosite by live *P. putida* MnB1 resulted in the oxidation of liberated Mn(II) in solution and formation of biogenic Mn oxides (Figs. 2 and 3). Mn oxides produced by *P. putida* MnB1 which used dissolved Mn^{2+} ions and natural rhodochrosite as the Mn(II) origin and synthetic δ-MnO_2 were analyzed by SEM-EDS (Fig. 2). SEM showed that a number of cells (the arrows) adhered to the surface of biogenic Mn oxides (Fig. 2a-d). XRD and SEM results indicated that biogenic Mn oxides were poorly ordered, poorly crystalline phyllomanganate, which was similar to δ-MnO_2, but varied in morphology (Figs. 2

and 3). EDS analysis showed that the biogenic and synthetic Mn oxides were mainly composed of O and Mn, and other elements as Fe, P and Mg.

LBB tests also supported the oxidation of Mn(II) (Fig. 4). In the sterile control and inactivated control, oxidation rates of natural and synthetic rhodochrosite were rather slow or the oxidation process was inhibited, which indicated that an abiotic oxidation process was thermodynamically favourable but at a rather low rate (Diem and Stumm, 1984). On the contrary, the presence of *P. putida* MnB1 caused a significant increase in Mn oxides concentration through the reaction time ($p<0.05$). For the natural rhodochrosite treatment, after reaction from 1 d to 7 d, the Mn oxide content increased from 6.28 ± 0.42 mg L^{-1} to 22.31 ± 5.31 mg L^{-1}. For the synthetic rhodochrosite treatment, at the end of the experiments (7d), Mn oxides content was 60.32 ± 5.20 mg L^{-1} in the presence of synthetic rhodochrosite, obviously higher than the natural rhodochrosite treatment. These results may be mainly attributed to the difference in crystal structure or the incorporation of foreign ions such as Al, Mg and Si (Böttcher and Dietzel, 2010; Prieto et al., 2013; Putnis and Ruiz-Agudo, 2013).

Fig. 4a and b shows the changes in dissolved Mn(II) concentration during reaction of *P. putida* MnB1 with natural and synthetic rhodochrosite. Mn(II) concentrations were significantly lower for live *P. putida* MnB1 treatments than the sterile control and the inactivated control ($p<0.05$). Over the entire reaction time, dissolved Mn(II) released from the natural rhodochrosite with a concentration of less than 0.5 mg L^{-1} was observed in the presence of live cells, while Mn(II) concentrations were significantly increased with respect to the inactivated cells treatment ($p<0.05$). This meant that live cells could effectively oxidize Mn(II) in solution to form Mn oxides, but abiotic dissolution of natural rhodochrosite only caused release of dissolved Mn(II) (Fig. 4) (Jensen et al., 2002; Luo and Millero, 2003). Overall, it was concluded that only live cells could effectively dissolve natural and synthetic rhodochrosite and subsequently oxidize liberated Mn(II) ions to form Mn oxides, while inactivated cell treatments or cell-free treatments did not contribute to the formation of Mn oxides.

3.2 Dissolution of natural rhodochrosite by bacterial EPS

The dissolution rate of natural rhodochrosite at various pHs, ionic strengths, EPS concentrations and rhodochrosite dosages with and without bacterial EPS are listed in Table 1. The dissolution rate of natural rhodochrosite by EPS was significantly increased at low pH conditions (pH=5.0) ($p<0.05$) in comparison with the EPS-free treatment. When the solution initial pH varied from 8.0 to 5.0, the dissolution rate for the control treatment was only increased about 1.2 times, however, in the presence of EPS, the rate was increased more than 26 times. Moreover, the dissolution rate was increased with EPS concentration under neutral conditions (pH=7.0). The dissolution rates were 0.055 ± 0.003, 0.075 ± 0.003 and 0.111 ± 0.018 μg Mn(II) min^{-1} with EPS concentrations of 0, 0.4 and 1.6 mg TOC L^{-1}, respectively. High levels of ionic strength (0.1 and 0.5 M NaCl) were favourable to an increase in Mn(II) concentration in the presence of 0.8 mg TOC L^{-1} EPS, and the dissolution rate increased by 15.6% as the ionic strength increased from 0.1 to 0.5 mol L^{-1}. For the EPS treatment, the dissolution rate of natural rhodochrosite also increased with the rhodochrosite dosage. In addition, EPS did not exhibit the ability to oxidize Mn^{2+} to Mn oxides during 5 d reaction (Fig. 5). These results indicate that bacterial EPS contributed to increasing dissolution of natural rhodochrosite, which was influenced by water chemistry factors, such as pH, EPS concentration and ionic strength. This suggested that EPS secreted by *P. putida* MnB1 cells played a significant role in enhancing the dissolution of natural rhodochrosite and subsequent release of Mn(II) for bacterial Mn oxidation ($p<0.05$).

3.3 Dissolution mechanism of natural rhodochrosite identified by FTIR

Oxidative dissolution of natural rhodochrosite to produce Mn oxides by fungi has been reported (Tang et al., 2013), however, little is known about the involvement of EPS in the dissolution of natural rhodochrosite. Functional groups of bacterial EPS involved in the dissolution of natural rhodochrosite were explored by FTIR spectroscopy (Fig. 6). For the purified EPS, the band at 3422 cm^{-1} was attributed to

O-H stretching in polysaccharides or protein groups and the band at 2931 cm^{-1} corresponded to C-H stretching (Braissant et al., 2007). The band at 1653 cm^{-1} was ascribed to the C=O stretching in amide I, while the band at 1541 cm^{-1} was confirmed as N-H bending in proteins (Guibaud et al., 2003; Guibaud et al., 2005). The band near 1400 cm^{-1} was identified as the symmetric stretching of C=O in COOH and the band at 1241 cm^{-1} was ascribed to N-H bending and C-N stretching vibrations (Nara et al., 1994; Omoike and Chorover, 2004). The band at 1038 cm^{-1} was mainly attributed to the stretching of C-O-C and C-H in polysaccharides (Guibaud et al., 2005; Comte et al., 2006; Zhang et al. 2006). After reaction with natural rhodochrosite, the bands at 1241 cm^{-1} and 1541 cm^{-1} disappeared, whereas the bands near 1653 cm^{-1} and 1400 cm^{-1} became much weaker. Besides, the bands near 2931 cm^{-1} and 1083 cm^{-1} became a doublet located at 2938 cm^{-1} and 2885 cm^{-1}, 1110 cm^{-1} and 1046 cm^{-1}, respectively. Overall, these results suggested that the functional groups of N-H in proteins, C=O in COOH or amide I and C-H or C-O-C in polysaccharides were involved in the dissolution of natural rhodochrosite. The strong Mn(II) binding ability of EPS to rhodochrosite might partly explain the enhanced dissolution of rhodochrosite in the presence of EPS. However, the detailed mechanism of EPS dissolution of natural rhodochrosite at water-mineral interfaces needs further study.

4 Conclusions

In this study, *P. putida* MnB1 cells could effectively dissolve natural and synthetic rhodochrosite and subsequently oxidize liberated Mn(II) ions to form Mn oxides, and EPS from the bacteria played an important role in enhancing the dissolution of rhodochrosite. The dissolution rate of natural rhodochrosite in the presence of EPS was significantly enhanced under acidic conditions. Other factors such as EPS concentration, ionic strength and rhodochrosite dosage also significantly affected the dissolution of natural rhodochrosite. FTIR spectroscopy indicated that the dissolution of natural rhodochrosite by EPS was mainly attributed to the involvement of N-H, C=O and C-H groups. This study demonstrates for the first time the important role of bacterial EPS in biotic dissolution and oxidation of natural rhodochrosite.

Acknowledgements

This work was supported by the National Natural Science Foundation of China (U1120302 and 21177127).

References

Bosecker, K.: Bioleaching: Metal solubilization by microorganisms, Fems Microbiol Rev, 20, 591-604, doi: 10.1111/j.1574-6976.1997.tb00340.x, 1997.

Braissant, O., Decho, A. W., Dupraz, C., Glunk, C., Przekop, K. M., and Visscher, P. T.: Exopolymeric substances of sulfate-reducing bacteria: Interactions with calcium at alkaline pH and implication for formation of carbonate minerals, Geobiology, 5, 401-411, doi: 10.1111/j.1472-4669.2007.00117.x, 2007.

Brewer, P. G., and Spencer, D. W.: Colorimetric Determination of Manganese in Anoxic Waters, Limnol Oceanogr, 16, 107-110, 1971.

Böttcher, M. E., and Dietzel, M.: Metal-ion partitioning during low-temperature precipitation and dissolution of anhydrous carbonates and sulphates ion partitioning in ambient-temperature aqueous systems. EMU Notes in Mineralogy, 10. Mineralogical Society, Twickenham, UK, pp. 139-187, doi: 10.1180/EMU-notes.10.4, 2010.

Comte, S., Guibaud, G., and Baudu, M.: Relations between extraction protocols for activated sludge extracellular polymeric substances (EPS) and EPS complexation properties Part I. Comparison of the efficiency of eight EPS extraction methods, Enzyme Microb Tech, 38, 237-245, doi: 10.1016/j.enzmictec.2005.06.016, 2006.

Diem, D., and Stumm, W.: Is Dissolved Mn^{2+} Being Oxidized by O_2 in Absence of Mn-Bacteria or Surface Catalysts, Geochim Cosmochim Ac, 48, 1571-1573, doi: 10.1016/0016-7037(84)90413-7, 1984.

Duckworth, O. W., and Martin, S. T.: Role of molecular oxygen in the dissolution of siderite and rhodochrosite, Geochim Cosmochim Ac, 68, 607-621, doi: 10.1016/S0016-7037(00)00464-2, 2004.

294 Fan, D. L., and Yang, P. J.: Introduction to and classification of manganese deposits of
295 China, Ore Geol Rev, 15, 1-13, doi: 10.1016/S0169-1368(99)00011-6, 1999.

296 Fowler, T. A., Holmes, P. R., and Crundwell, F. K.: Mechanism of pyrite dissolution in
297 the presence of Thiobacillus ferrooxidans, Appl Environ Microb, 65, 2987-2993,
298 1999.

299 Gehrke, T., Telegdi, J., Thierry, D., and Sand, W.: Importance of extracellular
300 polymeric substances from Thiobacillus ferrooxidans for bioleaching, Appl Environ
301 Microb, 64, 2743-2747, 1998.

302 Germann, K.: Deposition of Manganese and Iron Carbonates and Silicates in Liassic
303 Marls of the Northern Limestone Alps (Kalkalpen), International Union of Geological
304 Sciences, 3, 129-138, 1973.

305 Guibaud, G., Tixier, N., Bouju, A., and Baudu, M.: Relation between extracellular
306 polymers' composition and its ability to complex Cd, Cu and Pb, Chemosphere, 52,
307 1701-1710, doi: 10.1016/S0045-6535(03)00355-2, 2003.

308 Guibaud, G., Comte, S., Bordas, F., Dupuy, S., and Baudu, M.: Comparison of the
309 complexation potential of extracellular polymeric substances (EPS), extracted from
310 activated sludges and produced by pure bacteria strains, for cadmium, lead and nickel,
311 Chemosphere, 59, 629-638, doi: 10.1016/j.chemosphere.2004.10.028, 2005.

312 Hansel, C. M., Zeiner, C. A., Santelli, C. M., and Webb, S. M.: Mn(II) oxidation by an
313 ascomycete fungus is linked to superoxide production during asexual reproduction, P
314 Natl Acad Sci USA, 109, 12621-12625, doi: 10.1073/pnas.1203885109, 2012.

315 Jensen, D. L., Boddum, J. K., Tjell, J. C., and Christensen, T. H.: The solubility of
316 rhodochrosite ($MnCO_3$) and siderite ($FeCO_3$) in anaerobic aquatic environments, Appl
317 Geochem, 17, 503-511, doi: 10.1016/S0883-2927(01)00118-4, 2002.

318 Kim, D. G., Jiang, S., Jeong, K., and Ko, S. O.: Removal of 17 alpha-Ethinylestradiol
319 by Biogenic Manganese Oxides Produced by the Pseudomonas putida strain MnB1,
320 Water Air Soil Poll, 223, 837-846, doi: 10.1007/s11270-011-0906-6, 2012.

321 Lafferty, B. J., Ginder-Vogel, M., and Sparks, D. L.: Arsenite Oxidation by a Poorly
322 Crystalline Manganese-Oxide 1. Stirred-Flow Experiments, Environ Sci Technol, 44,
323 8460-8466, doi: 10.1021/Es102013p, 2010.

324 Learman, D. R., Voelker, B. M., Vazquez-Rodriguez, A. I., and Hansel, C. M.:
325 Formation of manganese oxides by bacterially generated superoxide, Nat Geosci, 4,
326 95-98, doi: 10.1038/Ngeo1055, 2011a.

327 Learman, D. R., Wankel, S. D., Webb, S. M., Martinez, N., Madden, A. S., and Hansel,
328 C. M.: Coupled biotic-abiotic Mn(II) oxidation pathway mediates the formation and
329 structural evolution of biogenic Mn oxides, Geochim Cosmochim Ac, 75, 6048-6063,
330 doi: 10.1016/j.gca.2011.07.026, 2011b.

331 Luo, Y. X., and Millero, F. J.: Solubility of rhodochrosite ($MnCO_3$) in NaCl solutions,
332 J Solution Chem, 32, 405-416, doi: 10.1023/A:1024568711020, 2003.

333 Madden, A. S., and Hochella, M. F.: A test of geochemical reactivity as a function of
334 mineral size: Manganese oxidation promoted by hematite nanoparticles, Geochim
335 Cosmochim Ac, 69, 389-398, doi: 10.1016/j.gca.2004.06.035, 2005.

336 Nara, M., Tasumi, M., Tanokura, M., Hiraoki, T., Yazawa, M., and Tsutsumi, A.:
337 Infrared Studies of Interaction between Metal-Ions and Ca^{2+}-Binding Proteins -
338 Marker Bands for Identifying the Types of Coordination of the Side-Chain COO-
339 Groups to Metal-Ions in Pike Parvalbumin (Pi=4.10), Febs Lett, 349, 84-88, doi:
340 10.1016/0014-5793(94)00645-8, 1994.

341 Okazaki, M., Sugita, T., Shimizu, M., Ohode, Y., Iwamoto, K., deVrinddeJong, E. W.,
342 deVrind, J. P. M., and Corstjens, P. L. A. M.: Partial purification and characterization
343 of manganese-oxidizing factors of Pseudomonas fluorescens GB-1, Appl Environ
344 Microb, 63, 4793-4799, 1997.

345 Okita, P. M.: Manganese Carbonate Mineralization in the Molango District, Mexico,
346 Econ Geol Bull Soc, 87, 1345-1366, 1992.

347 Omoike, A., and Chorover, J.: Spectroscopic study of extracellular polymeric

substances from Bacillus subtilis: Aqueous chemistry and adsorption effects, Biomacromolecules, 5, 1219-1230, doi: 10.1021/Bm034461z, 2004.

Pan, X. L.: Microbial extracellular polymeric substances: the ignored but crucial bio-interface affecting mobility of heavy metals in environment. Res. J. Biotechnol. 5, 3-4, 2010.

Paxman, M. B. L. S.: Modification of the lowry procedure for the analysis of proteolipid protein, Analytical Biochemistry, 47, 184-192, 1972.

Prieto, M., Astilleros, J. M., and Fernandez-Diaz, L.: Environmental remediation by crystallization of solid solutions, Elements, 9, 195-201, doi: 10.2113/gselements.9.3.195, 2013.

Rohwerder, T., Gehrke, T., Kinzler, K., and Sand, W.: Bioleaching review part A: Progress in bioleaching: fundamentals and mechanisms of bacterial metal sulfide oxidation, Appl Microbiol Biot, 63, 239-248, doi: 10.1007/s00253-003-1448-7, 2003.

Roy, S.: Genetic diversity of manganese deposition in the terrestrial geological record, Geological Society,London, Special Publications, 119, 5-27, 1997.

Putnis, C. V., and Ruiz-Agudo, E.: The mineral-water interface: where minerals react with the environment, Elements, 9, 177-182, doi: 10.2113/gselements.9.3.177, 2013.

Saha, S. K., and Brewer, C. F.: Determination of the Concentrations of Oligosaccharides, Complex Type Carbohydrates, and Glycoproteins Using the Phenol Sulfuric-Acid Method, Carbohyd Res, 254, 157-167, 1994.

Shiller, A. M., and Stephens, T. H.: Microbial manganese oxidation in the lower Mississippi River: Methods and evidence, Geomicrobiol J, 22, 117-125, doi: 10.1080/01490450590945924, 2005.

Spiro, T. G., Bargar, J. R., Sposito, G., and Tebo, B. M.: Bacteriogenic Manganese Oxides, Accounts Chem Res, 43, 2-9, doi: 10.1021/Ar800232a, 2010.

Tang, Y. Z., Zeiner, C. A., Santelli, C. M., and Hansel, C. M.: Fungal oxidative dissolution of the Mn(II)-bearing mineral rhodochrosite and the role of metabolites in

manganese oxide formation, Environ Microbiol, 15, 1063-1077, doi: 10.1111/1462-2920.12029, 2013.

Tebo, B. M., Johnson, H. A., McCarthy, J. K., and Templeton, A. S.: Geomicrobiology of manganese(II) oxidation, Trends Microbiol, 13, 421-428, doi: 10.1016/j.tim.2005.07.009, 2005.

Tributsch, H.: Direct versus indirect bioleaching, Hydrometallurgy, 59, 177-185, doi: 10.1016/S0304-386x(00)00181-X, 2001.

Villalobos, M., Toner, B., Bargar, J., and Sposito, G.: Characterization of the manganese oxide produced by Pseudomonas putida strain MnB1, Geochim Cosmochim Ac, 67, 2649-2662, doi: 10.1016/S0016-7037(03)00217-5, 2003.

Zhang, D. Y., Wang, J. L., Pan, X. L.: Cadmium sorption by EPSs produced by anaerobic sludge under sulfate-reducing conditions. J. Haz. Mater. 138, 589-593, doi: 10.1016/j.jhazmat.2006.05.092, 2006.

Zhang, D. Y., Lee, D. J., and Pan, X. L.: Desorption of Hg(II) and Sb(V) on extracellular polymeric substances: Effects of pH, EDTA, Ca(II) and temperature shocks, Bioresource Technol, 128, 711-715, doi:10.1016/j.biortech.2012.10.089, 2013.

Zhu, M. Q., Paul, K. W., Kubicki, J. D., and Sparks, D. L.: Quantum Chemical Study of Arsenic (III, V) Adsorption on Mn-Oxides: Implications for Arsenic(III) Oxidation, Environ Sci Technol, 43, 6655-6661, doi: 10.1021/Es900537e, 2009.

Table 1. Dissolution rates of rhodochrosite under various conditions. Data were means ± standard error (n=3) and significant levels between control and EPS treatments were indicated by asterisks ($p < 0.05$).

Experimental parameters	Rhodochrosite dosage (g L^{-1})	EPS concentration (mg TOC L^{-1})	Initial pH	Ionic strength (M)	Dissolution rates (μg Mn(II) min^{-1})
Initial pH	5	0	5.0	0.01	0.101 ± 0.001
	5	0.8	5.0	0.01	0.768 ± 0.181*
	5	0	7.0	0.01	0.055 ± 0.003
	5	0.8	7.0	0.01	0.106 ± 0.016*
	5	0	8.0	0.01	0.047 ± 0.004
	5	0.8	8.0	0.01	0.028 ± 0.015
Ionic strength	5	0	7.0	0.01	0.055 ± 0.003
	5	0.8	7.0	0.01	0.106 ± 0.016*
	5	0	7.0	0.1	0.081 ± 0.005
	5	0.8	7.0	0.1	0.141 ± 0.009*
	5	0	7.0	0.5	0.111 ± 0.005
	5	0.8	7.0	0.5	0.163 ± 0.002*
EPS concentration	5	0	7.0	0.01	0.055 ± 0.003
	5	0.4	7.0	0.01	0.075 ± 0.003*
	5	0.8	7.0	0.01	0.106 ± 0.016*
	5	1.6	7.0	0.01	0.111 ± 0.018*
Rhodochrosite dosage	2	0	7.0	0.01	0.059 ± 0.004
	2	0.8	7.0	0.01	0.088 ± 0.007*
	5	0	7.0	0.01	0.055 ± 0.003
	5	0.8	7.0	0.01	0.106 ± 0.016*
	10	0	7.0	0.01	0.057 ± 0.001
	10	0.8	7.0	0.01	0.107 ± 0.011*

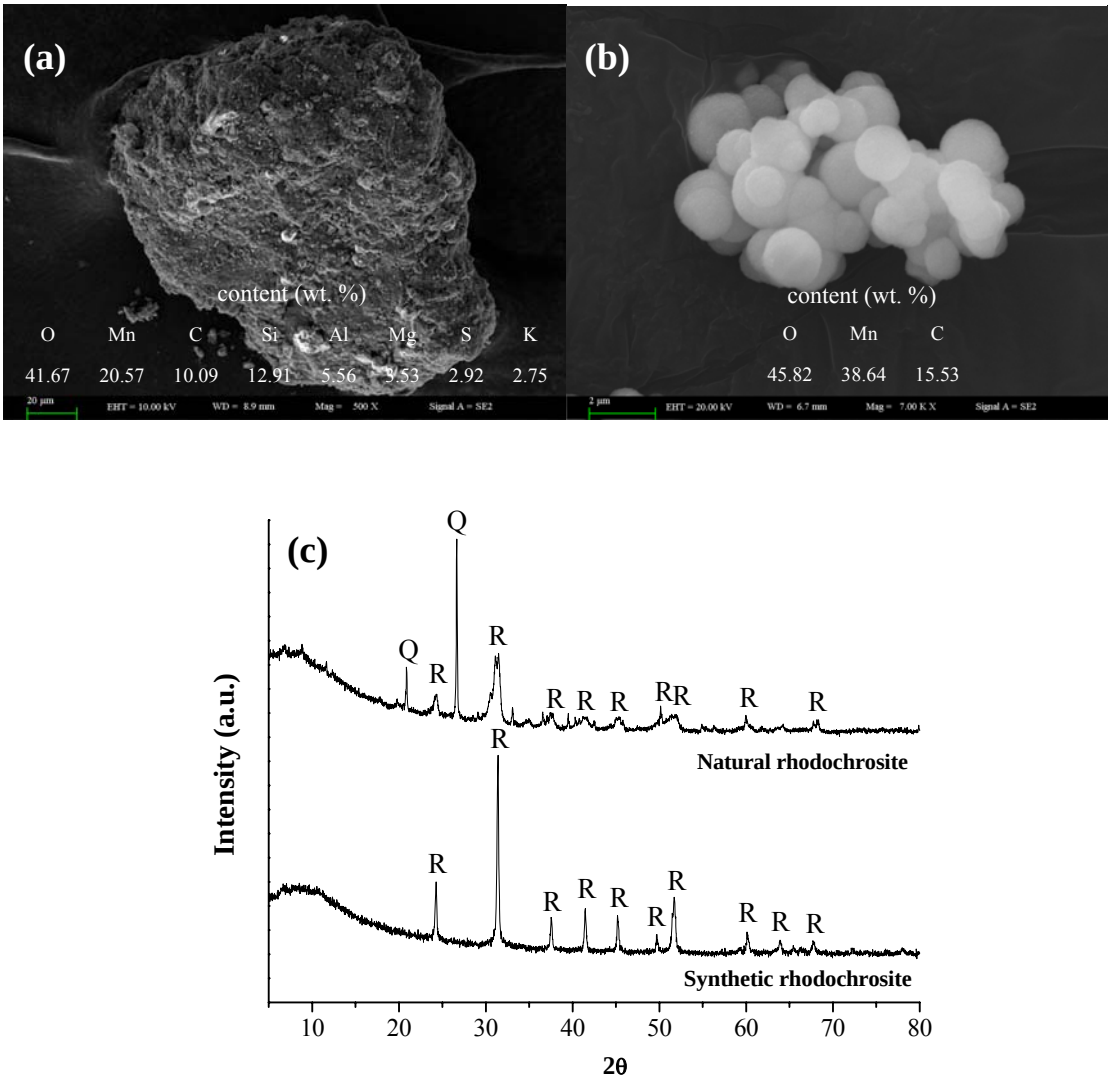

Fig. 1. SEM spectra of freshly natural rhodochrosite (a) and synthetic rhodochrosite (b); XRD patterns of natural and synthetic rhodochrosite (c) (R, Rhodochrosite; Q, Quartz)

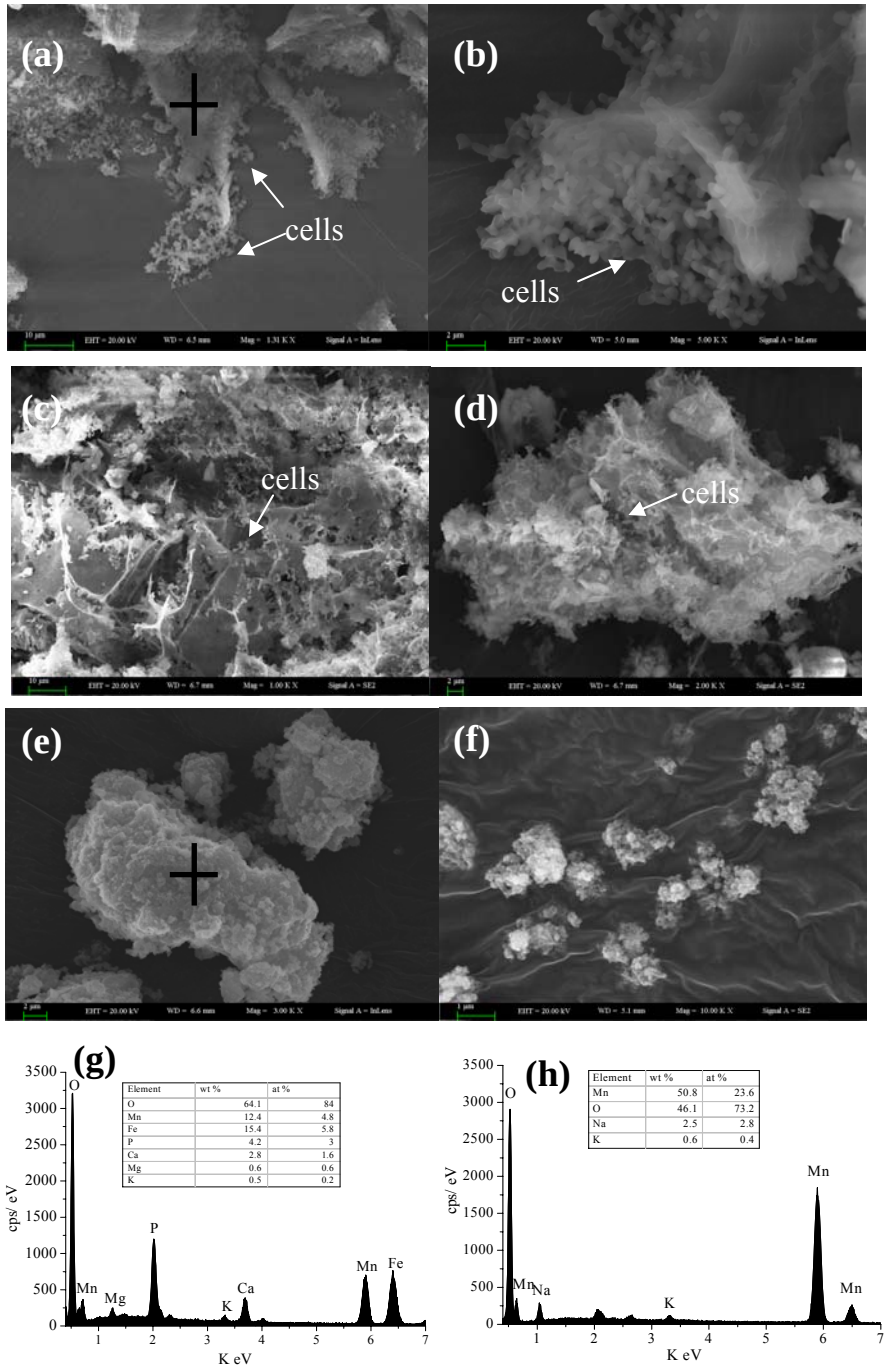

Fig. 2. SEM and EDS spectra of Mn oxides: 1) Biogenic Mn oxides using dissolved Mn^{2+} as Mn(II) origin (a, b); 2) Biogenic Mn oxides using natural rhodochrosite as Mn(II) origin (c, d); 3) freshly synthetic δ-MnO_2 (e, f); 4) EDS of biogenic Mn oxides (g) and freshly synthetic δ-MnO_2 (h). The "cross" represents the locality of the sample for EDS analysis.

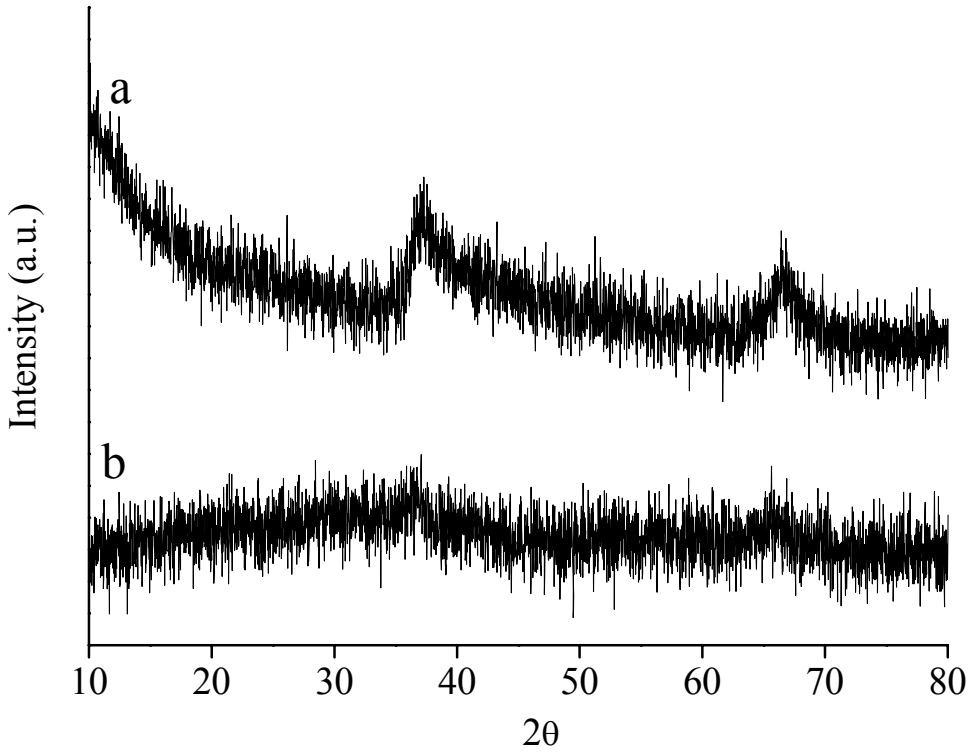

Fig. 3. Powder XRD patterns of synthetic δ-MnO_2 (a) and biogenic Mn oxides (b).

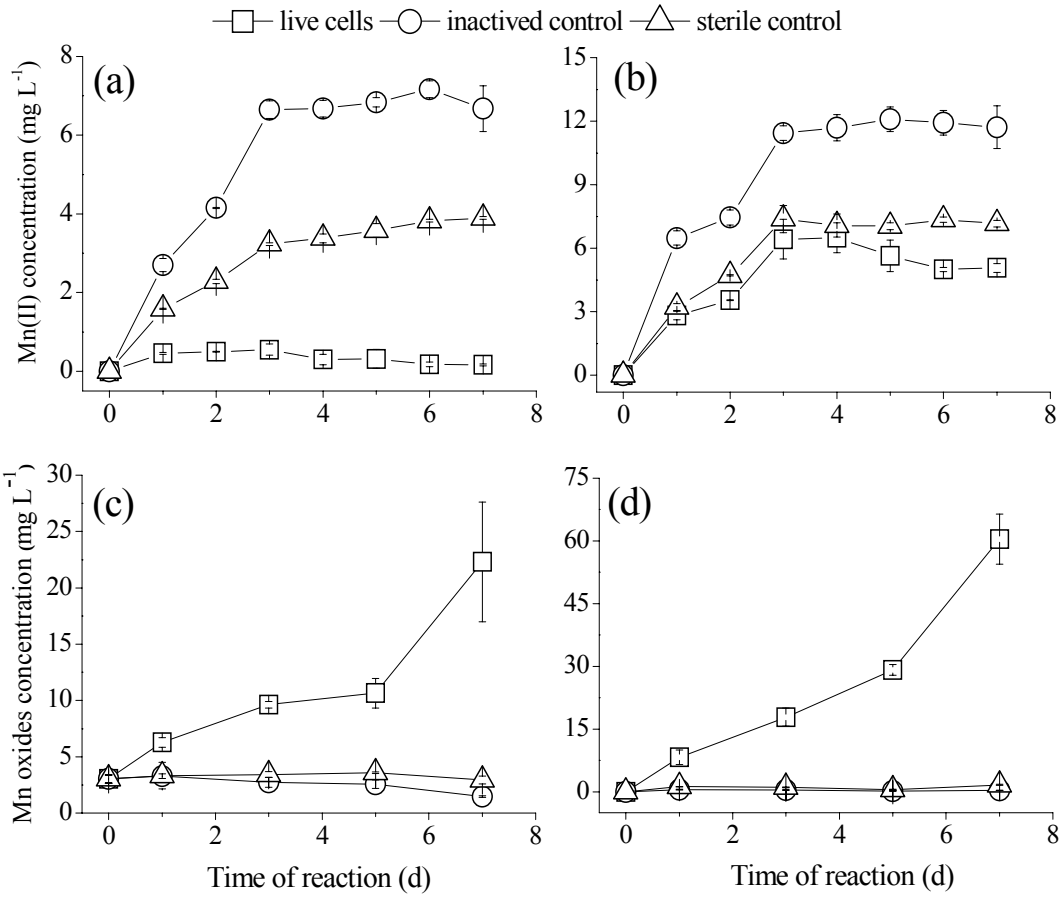

Fig. 4. Variation of Mn(II) concentration and Mn oxides as a function of reaction time during the dissolution of natural rhodochrosite (a, c) and synthetic rhodochrosite (b, d).

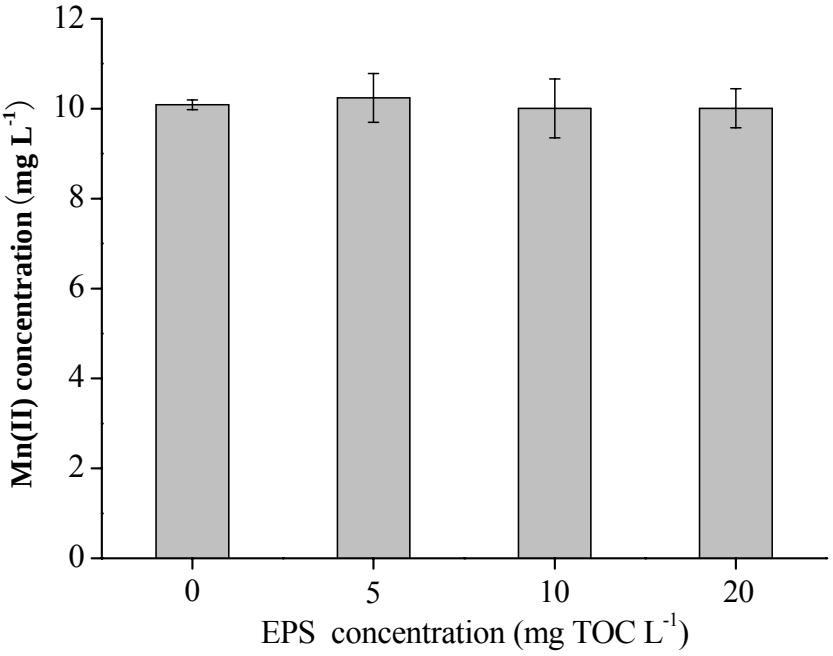

Fig. 5 Variation of Mn(II) concentration after reaction with bacterial EPS. The initial Mn(II) concentration was 10 mg L^{-1} and experimental conditions were 120 rpm for 5 days (25^{o}C).

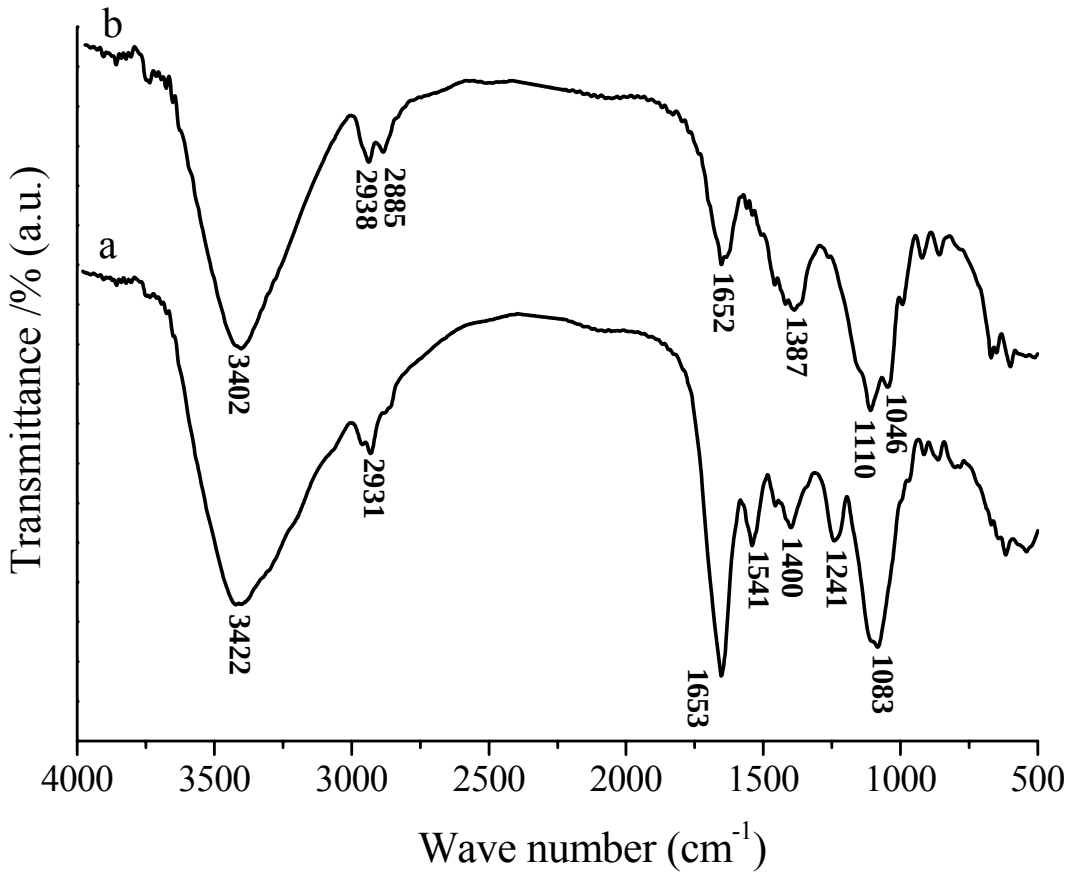

Fig. 6. Comparsion of FTIR spectra of EPS before and after reaction with natural rhodochrosite: **(a)** Pristine EPS; **(b)** EPS after reaction with natural rhodochrosite.